Nanoscale Advances



PAPER

View Article Online

View Journal | View Issue



Cite this: Nanoscale Adv., 2019, 1, 1826

Thermal effects on the surface plasmon resonance of Cu nanoparticles in phosphate glass: impact on Cu⁺ luminescence⁺

José A. Jiménez 1 ;*

An evaluation of the effects of temperature on the optical properties of phosphate glass containing Cu nanoparticles (NPs) and Cu^+ ions was carried out by means of optical absorption and photoluminescence (PL) spectroscopy measurements performed jointly *in situ* in the 298 to 573 K range. The surface plasmon resonance (SPR) of Cu NPs displayed a strong dampening effect with temperature, consistent with the thermal expansion of Cu NPs and an increase in the electron–phonon scattering rate. The PL of Cu^+ ions in the glass with Cu NPs showed the thermal quenching effect connected with an increase in non-radiative relaxation processes. Moreover, a comparison with the precursor glass without NPs revealed that a lower activation energy for the thermal quenching of Cu^+ PL results in the presence of Cu NPs for Cu^+ sites emitting in resonance with the SPR. It is suggested that the increase in electron–phonon interaction in Cu NPs with temperature impacts the PL quenching of Cu^+ ions the most. The current results suggest that a $Cu^+ \to Cu$ NP resonant energy transfer supports a deactivation of the Cu^+ emitting states with increasing temperature.

Received 10th December 2018 Accepted 12th March 2019

DOI: 10.1039/c8na00385h

rsc.li/nanoscale-advances

Introduction

Significant efforts have been devoted over the past decades to the fabrication of copper nanocomposite glasses and their characterization focusing on the plasmonic properties of interest to optical applications. 1-15 The preparation processes employed for doping the glass hosts with copper commonly involve a heat treatment (HT) step wherein the Cu nanoparticles (NPs) are precipitated. Given the difficulty intrinsic to the relatively high HT temperatures required for Cu particle development, the optical properties of such Cu nanocomposites are normally studied ex situ at relatively low temperatures, for instance at room temperature.1-15 Hence, studies on real-time isothermal monitoring of the optical properties of glasses undergoing Cu particle precipitation during HT are scarce.16-18 The study of the thermal effects on Cu NPs becomes further complicated by the propensity of neutral copper aggregates for undergoing oxidation. 19,20 Accordingly, a particular advantage of glass matrices for evaluating the optical properties of Cu NPs at high temperatures is the protective role of the solid host against Cu particle oxidation.

Department of Chemistry, University of North Florida, Jacksonville, FL 32224, USA. E-mail: jimenez.materials@gmail.com

In this context, Yeshchenko²¹ was able to study temperature effects on the surface plasmon resonance (SPR) of Cu NPs embedded in silica via the sol-gel route followed by annealing in reducing atmosphere. It was observed that the increase in temperature lead to the SPR red shift ascribed to thermal expansion in Cu NPs, and the broadening of the SPR which was attributed to the increase of the electron-phonon scattering rate with temperature.21 The theoretical framework was similarly employed to study the thermal effects on the SPR of Au NPs.22 On a subsequent work, an interesting study was conducted by Yeshchenko et al.²³ on the influence of temperature on the photoluminescence (PL) of the Cu nanocomposites also exhibiting plasmonic properties. In such case, the PL was assumed to arise from Cu NPs, wherein the PL quantum yield increased with temperature. It was argued that since the increase of temperature leads to the SPR red shift, this conduces to an increase in the spectral overlap with the PL favoring the plasmon enhancement factor along with a decrease of plasmon damping caused by interband transitions.23 Nevertheless, the temperature dependence of the optical properties of a glass containing a high concentration of both Cu NPs and luminescent Cu⁺ ions remains unexplored to the best of the author's knowledge. Accordingly, this work reports on an in situ optical characterization wherein the absorption and PL properties of Cu NP/Cu⁺-containing phosphate glass prepared by thermal processes were investigated jointly from 298 to 573 K. Whereas the Cu NPs exhibit aforementioned SPR dampening effect, the PL of Cu⁺ ions presents no enhancement but is rather shown to be quenched with temperature, and more drastically in

 $[\]dagger$ Electronic supplementary information (ESI) available. See DOI: 10.1039/c8na00385h

[‡] Present address: Functional Films Lab, BASF Corporation, 2655 Route 22 West, Union, NJ 07083, USA.

connection with the SPR peak of Cu NPs. The results are discussed in the context of the thermal effects of Cu NPs supporting a deactivation of the resonant Cu^+ emitting states with increasing temperature.

2. Experimental

Phosphate glasses were made with a BaO: P_2O_5 composition by the melt-quench technique as described elsewhere. Herein, the copper oxide dopant and reducing agent tin are added as 10 mol% of each CuO and SnO in relation to network former P_2O_5 . This melt-quenched glass is herein referred to as CuSn glass. Such glass has been shown to possess a high concentration of luminescent Cu^+ ions due to redox chemistry likely occurring in the melt^{24,25} as

$$2Cu^{2+} + Sn^{2+} \rightarrow 2Cu^{+} + Sn^{4+}$$
 (1)

The melt-quenched glass still shows some Cu^{2+} residues (estimated at $\sim\!2\%$ of the nominal amount of $CuO)^{25}$ which become evident from the absorption feature around 1.5 eV (see Fig. S1 of the ESI† file – obtained with Perkin-Elmer 35 UV/Vis spectrophotometer). In contrast to silver with most firmly oxidized state as $Ag^+,^{26-29}$ copper readily oxidizes to Cu^+ and Cu^{2+} ions where the latter possess relatively high stability under the melting in ambient atmosphere at high temperatures. This makes it challenging to eradicate all copper(π) in the melt. However, most copper ions in the CuSn precursor glass are indicated to exist as Cu^+ ions which becomes apparent from the substantial red shift in the UV absorption edge (Fig. S1†) owing to $3d^{10} \rightarrow 3d^94s^1$ transitions. Further, a subsequent HT of the glass allows for the effective precipitation of Cu NPs, 1,8,25 e.g. owing to a subsequent reduction of copper ions as

$$2Cu^{+} + Sn^{2+} \rightarrow 2Cu^{0} + Sn^{4+}$$
 (2)

In the present case, the Cu nanocomposite was obtained by HT performed at 733 K for a duration of 60 min, and is referred to herein as CuSn-NP glass. The Cu NPs grown in the phosphate glass matrix containing 10 mol% of each CuO and SnO by similar thermal processing have been inspected by transmission electron microscopy (TEM), and observed with an average diameter of about 2.5 nm. ¹⁶ Shown in Fig. 1 is a sample image obtained with a JOEL2010F transmission electron microscope. ¹⁶ Samples of the CuSn and CuSn-NP glasses were cut and polished in order to produce glass slabs with final thicknesses of about 1.0 mm, to be subjected to the optical measurements as described below.

Optical absorption and steady-state PL measurements were carried out jointly *in situ* with a CRAIC Technologies FLEX microspectrophotometer (MSP) equipped with mercury and xenon lamps, and a Linkam THMS600 temperature control stage. The temperatures are chosen from 298 to 573 K so that further Cu particle development during the measurements can be neglected. The samples were taken to the target temperatures at a rate of 50 K min⁻¹. Experiments were performed with a $10 \times$ objective on 97.4 μ m \times 97.4 μ m sample areas. Particular

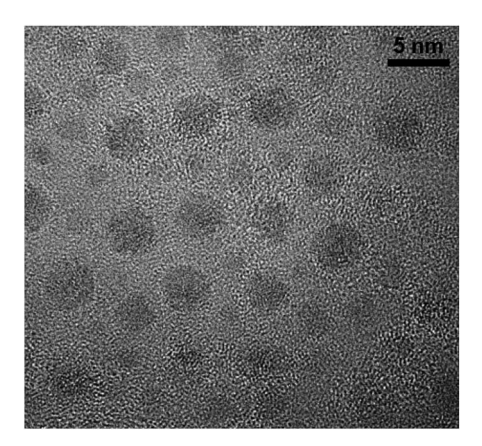


Fig. 1 TEM image of Cu NPs observed in plasmonic nanocomposite glass obtained by thermal processing of the CuSn precursor glass at 873 K for 1 h.

attention was given to keep the sampled area and all other conditions constant during the measurements. The PL spectra were recorded under excitation at 365 nm (3.40 eV). Herein, wavelength selection was realized by a band pass filter with full-width at half-maximum of about 45 nm.

Results and discussion

Fig. 2 shows optical absorption spectra obtained for the CuSn-NP glass within the 298 to 573 K range. The spectrum recorded at 298 K shows the typical profile of the embedded Cu NPs with a maximum in the vicinity of 2.16 eV (~574 nm).^{8,10,12,21,24} However, strong SPR suppression is observed with increasing temperature, primarily above 323 K. Following the method reported by Yeshchenko and co-workers for dielectric-embedded Cu NPs²¹ and Au NPs,²² the spectra were deconvoluted into two Lorentzian components aiming to separate the contribution of intraband (SPR) from the interband electronic transitions. As an example, the inset of Fig. 2 shows the deconvolution

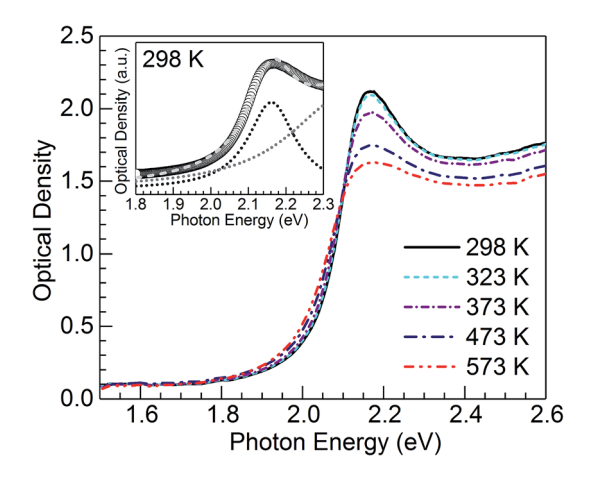


Fig. 2 Optical absorption spectra of the nanocomposite CuSn-NP glass obtained at displayed temperatures. The inset shows the spectrum for 298 K (open circles) deconvoluted into two Lorentzian components (dotted curves); the dashed trace is the cumulative fit.

Nanoscale Advances

performed on the spectrum recorded at 298 K. In this approach, the high-energy contribution is connected to the interband transitions in the metal, while the low-energy band corresponds to the SPR of Cu NPs.21 Hence, the latter can be adequately employed for the evaluation of the influence of temperature on SPR spectral features. The deconvolution results concerning SPR peak position and bandwidth for the spectra of the five temperatures in Fig. 2 are plotted in Fig. 3(a) and (b), respectively. The trends are apparent for the SPR red shift and also the broadening of the SPR band with the increase in temperature. From the linear fit to the SPR peak data in Fig. 3(a), the values for the intercept and slope were estimated at 2.186 (± 0.002) eV and $-7.8~(\pm 0.4) \times 10^{-5}~\text{eV}~\text{K}^{-1}$, respectively (correlation coefficient r = -0.996). Further, for the linear fit to the SPR bandwidth data in Fig. 3(b), the intercept and slope were 0.103 (± 0.002) eV and 1.65 $(\pm 0.04) \times 10^{-4}$ eV K⁻¹, respectively (r =0.999). Whereas the estimated intercepts correspond to lowtemperature extremes (0 K), the slopes designate the rates of change in the spectral properties with temperature in the examined range.

The trends observed in Fig. 3 are in good agreement with Yeshchenko²¹ who studied the temperature effects on the SPR

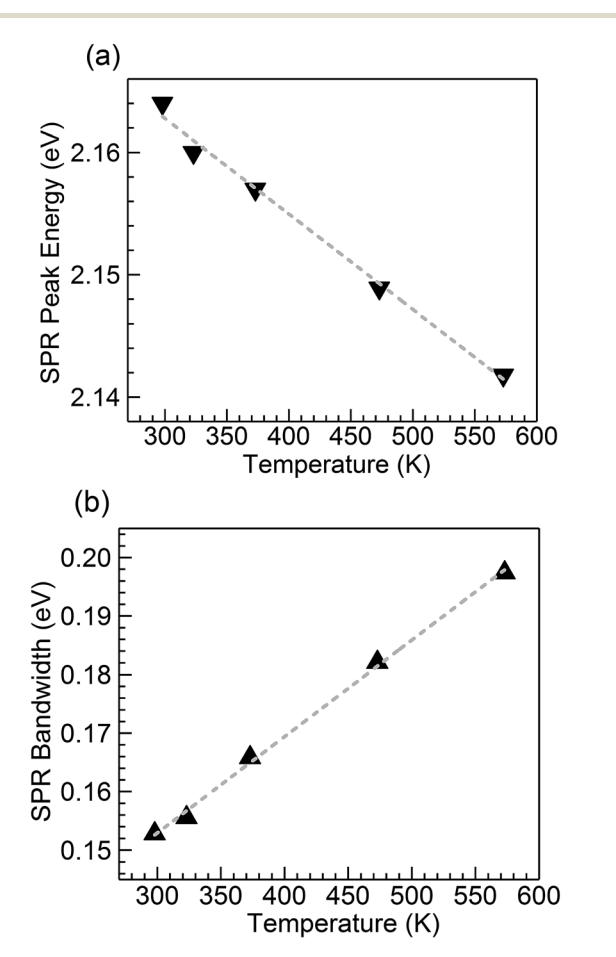


Fig. 3 Temperature dependence of (a) peak energy and (b) bandwidth of the SPR band resulting from the Lorentzian deconvolution of the absorption spectra for the nanocomposite CuSn-NP glass (Fig. 2); the dashed traces are linear fits to the data

of Cu NPs embedded in a silica matrix. Although the author examined a range in Cu particle sizes, it was noticed that the peak position and width trends were monotonic with the increase in temperature and were not qualitatively different amongst the sizes studied.21 Hence, in the present study the trends arising from thermal effects on the CuSn-NP glass may be likewise interpreted in the context of the thermal expansion in Cu NPs influencing the SPR red shift, and the increase of electron-phonon scattering rate affecting the bandwidth.21,22

Concerning the PL properties of the melt-quenched CuSn precursor glass, these have been previously studied at room temperature in ref. 25. It has been observed that shortwavelength excitation (e.g. 260 nm) produces broad band emission having a significant contribution from divalent tin centers, whereas increasing excitation wavelength leads to an emission red shift owing to the growing contribution from Cu⁺ ions in connection with $3d^94s^1 \rightarrow 3d^{10}$ transitions. In the end, excitation at 360 nm and longer wavelengths produces the broad band emission which arises solely from the monovalent copper ions.25 The Cu⁺ emitting states (T_{1g}, T_{2g}) are interpreted as arising from spin-orbit coupling of the excited triplet state (3Eg) which is populated by intersystem crossing from the excited singlet state of the 3d⁹4s¹ configuration.³⁰ In Fig. 4, the PL of Cu⁺ ions in the CuSn-NP glass is examined at 298 K in comparison with that of the CuSn glass under the excitation at 365 nm (3.40 eV) in the MSP. A depressed band is obtained for the heat-treated CuSn-NP glass, which is expected in accord with a depletion of copper ions due to their reduction, e.g. via eqn (2), leading to the precipitation of the Cu NPs. In addition, a dip is observed near 2.16 eV in good agreement with the position of the SPR of Cu NPs in the glass (Fig. 2). This effect is related to a resonant energy transfer from the monovalent copper ions to the NPs, i.e. photon-reabsorption or cascade-type energy transfer also observed in a similar Cu nanocomposite.8

The temperature dependence of Cu⁺ PL in the CuSn glass has been studied in the 298-573 K range, and compared with that of analogous glasses co-doped with either Sm³⁺ or Nd³⁺ where the

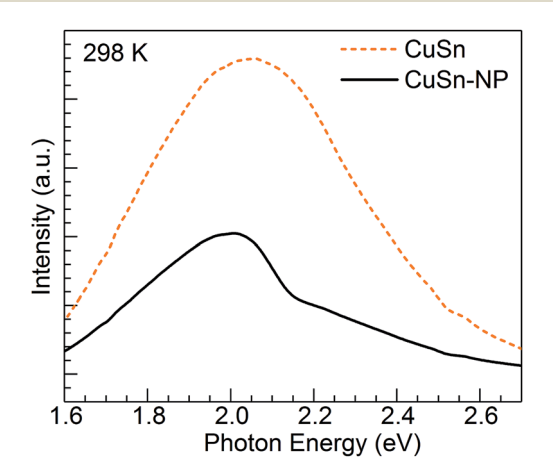


Fig. 4 PL emission spectra obtained for the CuSn precursor glass and the CuSn-NP nanocomposite at 298 K.

Nanoscale Advances Paper

results were analyzed in the context of glass structure.31 Herein, an attempt is made to evaluate the influence of the plasmonic Cu particles on the temperature dependence of Cu⁺ PL in the CuSn-NP glass. Thus, shown in Fig. 5 are PL emission spectra of the CuSn-NP nanocomposite glass obtained in the 298-573 K range. The absorption spectrum for the CuSn-NP glass at 298 K is overlaid to demonstrate the matching between the SPR of Cu NPs and the dip observed in the emission band around 2.16 eV. Clearly, the PL decreases with increasing temperature, as opposed to the report by Yeshchenko et al. 23 wherein the PL was assumed to arise from Cu NPs and the quantum yield increased with temperature. In the current system no PL enhancement is observed, but rather the thermal quenching of the broad Cu⁺ emission band is exhibited concurring with the increase in the non-radiative processes depopulating the Cu⁺ emitting states.31-33 The excited states of the luminescent ions in the solid host decay non-radiatively by exciting lattice vibrations, i.e. by phonon emission. With increasing temperature of the solid, the ion-lattice interaction becomes stronger and the probability for non-radiative relaxation of the ions increase. This results in the PL quenching effect observed. Henceforth, an evaluation of the thermal stability of Cu⁺ PL in the CuSn-NP glass is pursued in comparison to the CuSn glass, and focusing on Cu⁺ sites emitting in resonance with the SPR of Cu NPs.

The PL quenching with temperature may be assessed in the context of

$$I(T) = \frac{I_0}{[1 + c \exp(-E_A/k_B T)]}$$
 (3)

where I(T) is the emission intensity at a given temperature, I_0 is the initial intensity, c is a constant, $k_{\rm B}$ is Boltzmann's constant and E_A is the activation energy for the thermal quenching.^{31–33} Eqn (3) can be linearized as

$$\ln\left[\frac{I_0}{I(T)} - 1\right] = \frac{-E_A}{k_B T} + \ln c \tag{4}$$

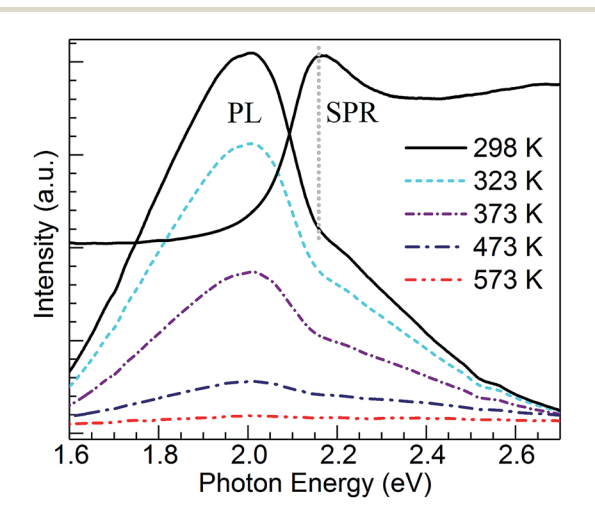
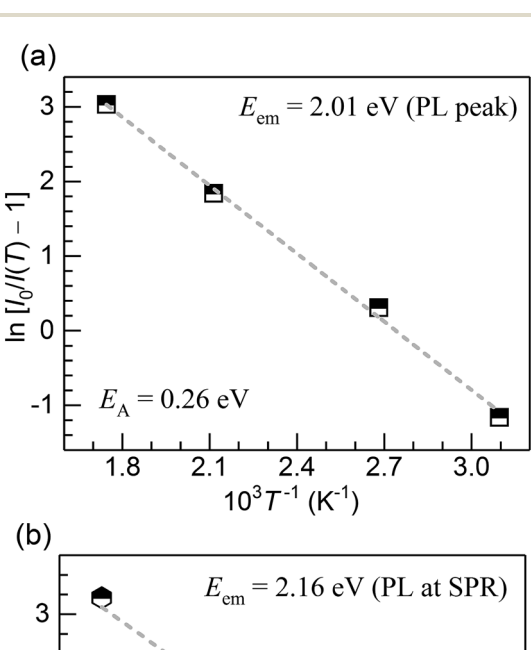


Fig. 5 PL emission spectra of the nanocomposite CuSn-NP glass obtained at displayed temperatures. The absorption spectrum for the glass at 298 K is overlaid to show the matching between the SPR and the dip observed in the PL spectra around 2.16 eV.

so a plot of $\ln[I_0/I(T) - 1] vs$. reciprocal temperature can be used for estimating the corresponding activation energy. In this framework, the thermal quenching of Cu⁺ PL was assessed for the CuSn glass for an emission intensity near the peak in the broad Cu⁺ band, where the activation energy was estimated at $0.256 \ (\pm 0.004) \ \text{eV}$. Herein, the path of $\text{Cu}^+ \rightarrow \text{Cu NP energy}$ transfer is further explored as potential contributor to the PL thermal quenching in the CuSn-NP glass by evaluating the emission intensity for Cu⁺ in resonance with the SPR. Thus, Fig. 6 shows the corresponding plots of $\ln[I_0/I(T) - 1]$ vs. reciprocal temperature obtained for the CuSn-NP glass for Cu⁺ emission energy monitored at (a) 2.01 eV (PL peak), and (b) 2.16 eV (matching the SPR peak). The data showed linear relationships (correlation coefficients r of -0.999 for both) in agreement with eqn (4). From the slopes obtained by linear regression analyses, the activation energies determined are $0.262 (\pm 0.010)$ and $0.181 (\pm 0.010)$ eV for Cu⁺ emission monitored at 2.01 and 2.16 eV, respectively. An analogous evaluation was performed for the CuSn glass as reference, yielding activation energies of 0.256 (± 0.004) and 0.242 (± 0.005) eV for the emission at 2.01 and 2.16 eV, respectively (data shown in



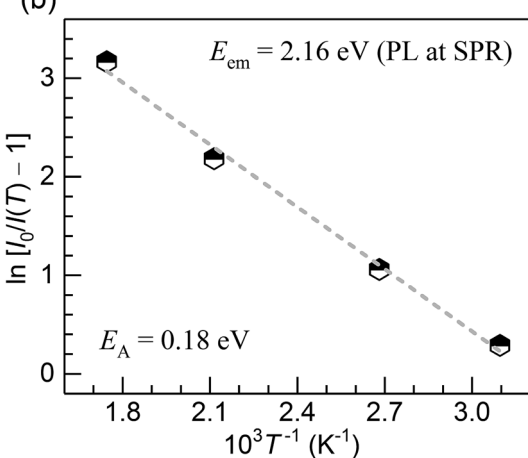


Fig. 6 Plots of $ln[I_0/I(T) - 1]$ vs. reciprocal temperature for CuSn-NP glass obtained for the Cu⁺ photon emission energy being monitored at (a) 2.01 eV (PL peak), and (b) 2.16 eV (matching SPR); the dashed lines are the linear fits to the data

Nanoscale Advances Paper

Fig. S2 of the ESI† file). The results are all plotted together in Fig. 7 for a graphic appraisal. It can be easily recognized that while the CuSn and CuSn-NP glasses exhibit similar values (within error) for the emission near the PL maximum at 2.01 eV, the CuSn-NP glass exhibits markedly a decrease for emission at 2.16 eV in resonance with the SPR peak of Cu NPs. The results then point toward a significant influence from the Cu NPs decreasing the thermal stability of the Cu⁺ emission in correspondence with a $Cu^+ \rightarrow Cu$ NP resonant energy

The Cu⁺ luminescence quenching with temperature being similar for the CuSn and CuSn-NP glasses for the emission evaluated near the maximum (to the low energy side of SPR, see Fig. 5) appears connected to the glass matrix itself. In a solid host, the most energetic vibrations are mainly responsible for the radiationless processes. In phosphate glasses, these are the stretching vibrations between phosphorus atoms and the non-bridging oxygens in the glass network, typically manifested around 1200 cm⁻¹.34 It can be then realized that the deactivation pathway brought in by the fundamental increase in Cu+ ion-lattice interaction with temperature is the dominant cause for the out-of-resonance thermal quenching of the Cu⁺ PL.³¹ However, in the present work additional evidence is provided in support of a different quenching route, namely the $Cu^+ \rightarrow Cu$ NP resonant transfer which may become more effective with the increase in temperature. Herein, the SPR peak position variation was not as pronounced as the bandwidth increase, as perceived from the assessment of data in Fig. 2. In particular, the latter effect has been connected with an increase in the electron-phonon interactions in the NPs.21 The electron-phonon scattering processes within the NPs, as well as electron-electron interactions, are part of the ultrafast relaxation processes in NPs which occur in the sub-picosecond to picosecond time scales.35 Ultimately, particle-matrix energy transfer processes result in the complete non-radiative relaxation of the nanocomposite on a longer time scale.36 Accordingly, in Fig. 8 an attempt is made to represent the proposed thermal deactivation pathway of Cu⁺ ions emitting in resonance with the SPR of

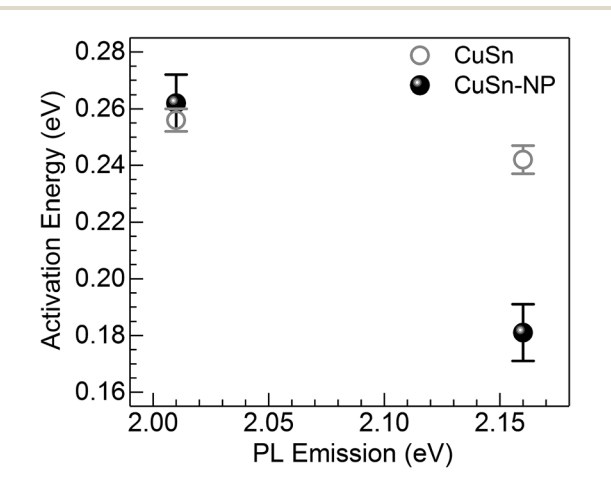


Fig. 7 Activation energy for the thermal quenching of Cu⁺ PL in the CuSn and CuSn-NP glasses vs. the photon energy of the PL emission.

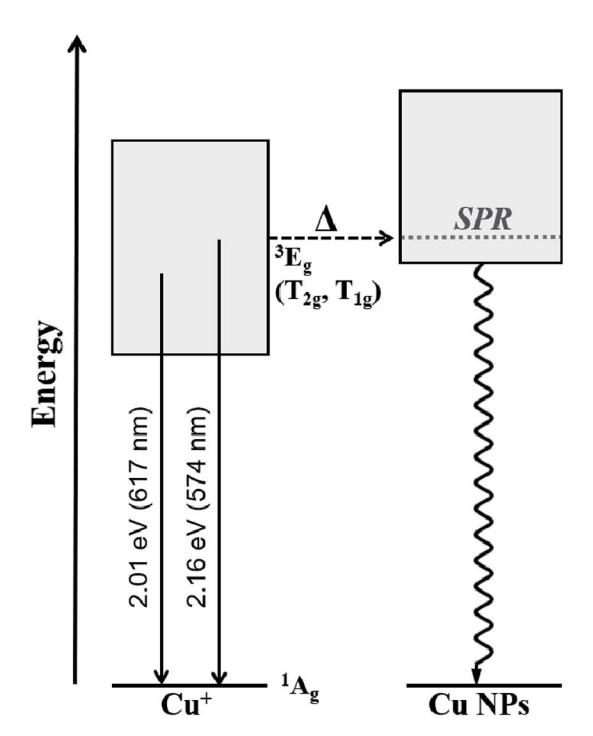


Fig. 8 Schematic representation for the proposed thermal deactivation pathway (Δ) of Cu⁺ ions emitting in resonance with the SPR of Cu NPs in the glass host. Vertical solid-straight and solid-curved arrows indicate radiative and non-radiative relaxation from Cu⁺ ions and Cu NPs, respectively

Cu NPs in the glass host. It is herein considered that the Cu⁺ sites with emitting states (T_{1g}, T_{2g}) in resonance with the SPR may transfer the energy to the Cu NPs wherein a complete nonradiative relaxation can take place through aforementioned relaxation processes involving the NPs.

Conclusions 4.

To summarize, a joint in situ assessment was performed on the influence of temperature in the 298 to 573 K range on the optical absorption and luminescence of barium-phosphate glass containing plasmonic Cu particles and Cu⁺ ions. The thermal effects on the SPR of Cu NPs were analyzed following the approach of deconvoluting the spectra into two Lorentzian components, where the one at lower energy is related to the plasmonic absorption (intraband) while the high-energy contribution is assumed for interband transitions. The strong suppression of the SPR absorption with temperature was manifest, concurring with the thermal expansion of Cu NPs influencing peak position and an increase in the electronphonon scattering rate producing band broadening. On the other hand, the PL of Cu⁺ ions showed no enhancement, but rather displayed the thermal quenching effect expected for an increase in non-radiative relaxation processes. In the general sense, this is associated with ion-lattice interactions likely supported by high-energy phonons in connection with nonbridging oxygens in the phosphate matrix. However, a lower activation energy for the thermal quenching of Cu⁺ PL was

Paper Nanoscale Advances

estimated in the presence of Cu NPs (~0.06 eV lower than the precursor glass) for Cu⁺ sites emitting in resonance with the SPR. It is then suggested that in the presence of Cu NPs in the glass, the Cu⁺ ions may experience the thermally-induced excited-state depopulation through two different channels: (i) the deactivation route brought in by the inherent increase in Cu⁺ ion-lattice interaction with temperature; and (ii) via the Cu⁺ → Cu NP resonant energy transfer, wherein the increase in electron-phonon interaction in Cu NPs with temperature supports an additional energy sink facilitated by non-radiative relaxation in the NPs and finalizing with energy exchange with the matrix.

Conflicts of interest

The author declares no conflict of interest.

Acknowledgements

The author is grateful to Dr Mariana Sendova from the Optical Spectroscopy & Nano-Materials Lab at New College of Florida for support with TEM work carried out at the Major Analytical Instrumentation Center at University of Florida.

References

- 1 K. Uchida, S. Kaneko, S. Omi, C. Hata, H. Tanji, Y. Asahara, A. J. Ikushima, T. Tokisaki and A. Nakamura, Optical nonlinearities of a high concentration of small metal particles dispersed in glass: copper and silver particles, J. Opt. Soc. Am. B, 1994, 11, 1236-1243.
- 2 G. De, M. Gusso, L. Tapfer, M. Catalano, F. Gonella, G. Mattei, P. Mazzoldi and G. Battaglin, Annealing behavior of silver, copper, and silver-copper nanoclusters in a silica matrix synthesized by the sol-gel technique, J. Appl. Phys., 1996, 80, 6734-6739.
- 3 A. Edgar, Strong red-light scattering from colloidal copper in ZBLAN fluoride glass, J. Non-Cryst. Solids, 1997, 220, 78-84.
- 4 B. Karthikeyan, M. Anija, C. S. Suchand Sandeep, T. M. Muhammad Nadeer and R. Philip, Optical and nonlinear optical properties of copper nanocomposite glasses annealed near the glass softening temperature, Opt. Commun., 2008, 281, 2933-2937.
- 5 R. Kibar, A. Cetin and N. Can, Effect of thermal treatment on linear optical properties of Cu nanoclusters, Phys. B, 2009, 404, 105-110.
- 6 Y. Teng, B. Qian, N. Jiang, Y. Liu, F. Luo, S. Ye, J. Zhou, B. Zhu, H. Zeng and J. Qiu, Light and heat driven precipitation of copper nanoparticles inside Cu²⁺-doped borate glasses, Chem. Phys. Lett., 2010, 485, 91-94.
- 7 D. Manzani, J. M. P. Almeida, M. Napoli, L. De Boni, M. Nalin, C. R. M. Afonso, S. J. L. Ribeiro and C. R. Mendonça, Nonlinear optical properties of tungsten lead-pyrophosphate glasses containing metallic copper nanoparticles, Plasmonics, 2013, 8, 1667-1674.

- 8 J. A. Jiménez, Optical properties of Cu nanocomposite glass obtained via CuO and SnO co-doping, Appl. Phys. A, 2014, 114, 1369-1376.
- 9 D. F. Franco, A. C. Sant'Ana, L. F. C. De Oliveira and M. A. P. Silva, The Sb₂O₃ redox route to obtain copper nanoparticles in glasses with plasmonic properties, I. Mater. Chem. C, 2015, 3, 3803-3808.
- 10 J. A. Jiménez, Silicon as reducing agent for controlled production of plasmonic copper nanocomposite glasses: a spectroscopic study, J. Electron. Mater., 2015, 44, 1369-1376.
- 11 W. Xiang, H. Gao, L. Ma, X. Ma, Y. Huang, L. Pei and X. Liang, Valence state control and third-order nonlinear optical properties of copper embedded in sodium borosilicate glass, ACS Appl. Mater. Interfaces, 2015, 7, 10162-10168.
- 12 J. A. Jiménez, Carbon as reducing agent for the precipitation of plasmonic Cu particles in glass, J. Alloys Compd., 2016, **656**, 685-688.
- 13 M. Nogami, N. T. T. An, V. X. Quang, Y. Kato and Y. Matsuoka, One-step fabrication of Cu nanoparticles on silicate glass substrates for surface plasmonic sensors, I. Non-Cryst. Solids, 2018, 495, 95-101.
- 14 P. Kumar, M. C. Mathpal and H. C. Swart, Multifunctional properties of plasmonic Cu nanoparticles embedded in a glass matrix and their thermodynamic behavior, J. Alloys Compd., 2018, 747, 530-542.
- 15 G. K. Inwati, Y. Rao and M. Singh, Thermodynamically induced in situ and tunable Cu plasmonic behaviour, Sci. Rep., 2018, 8, 3006.
- 16 M. Sendova, J. A. Jiménez, R. Smith and N. Rudawski, Kinetics of copper nanoparticle precipitation in phosphate glass: an isothermal plasmonic approach, Phys. Chem. Chem. Phys., 2015, 17, 1241-1246.
- 17 J. A. Jiménez, Carbon-promoted in situ evolution of Cu nanoclusters influencing Eu³⁺ photoluminescence in glass: bidirectional energy transfer, J. Phys. Chem. C, 2016, 120,
- 18 J. A. Jiménez, Carbon-driven synthesis of bi-plasmonic Ag-Cu nanocomposite phosphate glasses, Mater. Chem. Phys., 2018, **205**, 518-521.
- 19 M. D. Susman, Y. Feldman, T. A. Bendikov, A. Vaskevich and I. Rubinstein, Real-time plasmon spectroscopy study of the solid-state oxidation and Kirkendall void formation in copper nanoparticles, Nanoscale, 2017, 9, 12573-12589.
- 20 A. P. LaGrow, M. R. Ward, D. C. Lloyd, P. L. Gai and E. D. Boyes, Visualizing the Cu/Cu₂O interface transition in nanoparticles with environmental scanning transmission electron microscopy, J. Am. Chem. Soc., 2017, 139, 179-185.
- 21 O. A. Yeshchenko, Temperature effects on the surface plasmon resonance in copper nanoparticles, Ukr. J. Phys., 2013, 58, 249-259.
- 22 O. A. Yeshchenko, I. S. Bondarchuk, V. S. Gurin, I. M. Dmitruk and A. V. Kotko, Temperature dependence of the surface plasmon resonance in gold nanoparticles, Surf. Sci., 2013, 608, 275-281.

23 O. A. Yeshchenko, I. S. Bondarchuk and M. Yu. Losytskyy, Surface plasmon enhanced photoluminescence from copper nanoparticles: influence of temperature, *J. Appl. Phys.*, 2014, 116, 054309.

Nanoscale Advances

- 24 J. A. Jiménez and J. B. Hockenbury, Spectroscopic properties of CuO, SnO, and Dy₂O₃ co-doped phosphate glass: from luminescent material to plasmonic nanocomposite, *J. Mater. Sci.*, 2013, **48**, 6921–6928.
- 25 J. A. Jiménez, Efficient stabilization of Cu⁺ ions in phosphate glasses *via* reduction of Cu²⁺ by Sn²⁺ during ambient atmosphere melting, *J. Mater. Sci.*, 2014, **49**, 4387–4393.
- 26 J. A. Jiménez, M. Sendova and K. McAlpine, Revealing oxidation kinetics of dielectric-embedded Ag nanoparticles *via in situ* optical microspectroscopy, *Chem. Phys. Lett.*, 2012, **523**, 107–112.
- 27 P. Kumar, M. C. Mathpal, A. K. Tripathi, J. Prakash, A. Agarwal, M. M. Ahmad and H. C. Swart, Plasmonic resonance of Ag nanoclusters diffused in soda-lime glasses, *Phys. Chem. Chem. Phys.*, 2015, 17, 8596–8603.
- 28 R. Ma, J. Zhao, X. Chen, X. Qiao, X. Fan, J. Du and X. Zhang, Stabilization of ultra-small [Ag₂]²⁺ and [Ag_m]ⁿ⁺ nano-clusters through negatively charged tetrahedrons in oxyfluoride glass networks: to largely enhance the luminescence quantum yields, *Phys. Chem. Chem. Phys.*, 2017, 19, 22638–22645.
- 29 P. Kumar, M. C. Mathpal, J. Prakash, S. Hamad, S. V. Rao, B. C. Viljoen, M.-M. Duvenhage, E. G. Njoroge, W. D. Roos and H. C. Swart, Study of tunable plasmonic, photoluminescence, and nonlinear optical behavior of Ag

- nanoclusters embedded in a glass matrix for multifunctional applications, *Phys. Status Solidi A*, 2019, **216**, 1800768.
- 30 M. A. García, E. Borsella, S. E. Paje, J. Llopis, M. A. Villegas and R. Polloni, Luminescence time decay from Cu⁺ ions in sol-gel silica coatings, *J. Lumin.*, 2001, **93**, 253–259.
- 31 J. A. Jiménez, Temperature dependence of Cu⁺ luminescence in barium–phosphate glasses: effect of rare-earth ions (Sm³⁺, Nd³⁺) and correlation with glass structure, *J. Non-Cryst. Solids*, 2016, 432, 227–231.
- 32 J. A. Jiménez, Emission properties and temperature dependence of Cu⁺ luminescence in the CaO-CaF₂-P₂O₅ ternary glass system co-doped with CuO and SnO, *J. Phys. Chem. Solids*, 2015, **85**, 212–217.
- 33 E. Borsella, A. Dal Vecchio, M. A. García, C. Sada, F. Gonella, R. Polloni, A. Quaranta and L. J. G. W. van Wilderen, Copper doping of silicate glasses by the ion-exchange technique: a photoluminescence spectroscopy study, *J. Appl. Phys.*, 2002, **91**, 90–98.
- 34 R. Reisfeld, in *Radiationless Processes*, ed B. Di Bartolo, Plenum Press, New York, 1980.
- 35 C. Voisin, N. Del Fatti, D. Christofilos and F. Vallée, Ultrafast electron dynamics and optical nonlinearities in metal nanoparticles, *J. Phys. Chem. B*, 2001, **105**, 2264–2280.
- 36 J. A. Jiménez, S. Lysenko, V. S. Vikhnin and H. Liu, Interfacial effects in the relaxation dynamics of silver nanometal-glass composites probed by transient grating spectroscopy, *J. Electron. Mater.*, 2010, **39**, 138–143.